

## Optical properties of the 1:2 compound of dimethylferrocenium with tetracyanoquinodimethanide: $[(\text{Me}_2\text{Fc})(\text{TCNQ})_2]$

R. P. McCall

*Department of Physics, University of Southern Mississippi, Hattiesburg, Mississippi 39406*

D. B. Tanner

*Department of Physics, University of Florida, Gainesville, Florida 32611*

J. S. Miller

*Central Research and Development Department, E.I. du Pont de Nemours and Company, Inc.,  
Wilmington, Delaware 19898*

A. J. Epstein

*Department of Physics and Department of Chemistry, The Ohio State University, Columbus, Ohio 43210*

(Received 2 September 1986)

We present the results of a study of the room-temperature polarized reflectance of (1:2) 1,1'-dimethylferrocenium ditetracyanoquinodimethanide  $[(\text{Me}_2\text{Fc})(\text{TCNQ})_2]$  over the range between the far infrared and the near ultraviolet. Kramers-Kronig analysis of the reflectance is used to determine the optical properties of the compound. Vibrational features are evident at low frequencies whereas electronic excitations, including charge transfer between TCNQ molecules, are observed at higher frequencies.

### I. INTRODUCTION

The charge-transfer salts of 7,7,8,8-tetracyanoquinodimethane (TCNQ) have anisotropic structural, electrical, optical, and magnetic properties. The structure of the highly conducting salts, with conductivities  $\sigma$  at 300 K in the  $10\text{--}100\text{-}\Omega^{-1}\text{cm}^{-1}$  range, generally consists of one-dimensional chains of equally-spaced TCNQ molecules. In other salts, the TCNQ molecules have unequal separations—they appear as dimers, trimers, tetramers, etc. These salts have conductivities which are much lower:  $\sigma(300\text{ K}) = 10^{-5}\text{--}10\text{-}\Omega^{-1}\text{cm}^{-1}$ .

The structure<sup>1</sup> of (1:2) 1,1'-dimethylferrocenene- $(\text{TCNQ})_2$ , or  $(\text{Me}_2\text{Fc})(\text{TCNQ})_2$ , is triclinic, with segregated chains of TCNQ molecules and of  $\text{Me}_2\text{Fc}$  donor molecules [which consist of an iron ion  $\text{Fe}^{2+}$  sandwiched between two methylcyclopentadienyl ( $\text{CH}_3\text{C}_5\text{H}_4^-$ ) molecular ions]. These chains are parallel to the crystallographic  $b$  axis. The TCNQ units are equally spaced along the chain, but the two TCNQ molecules in each unit cell are crystallographically distinct in that the extracyclic double C—C bonds are different. However resonance Raman measurements<sup>1</sup> indicate that all TCNQ molecules possess a charge of  $0.42 \pm 0.10$ .

It has been proposed<sup>1</sup> that the alternating bond lengths may be due to the presence of a Peierls gap stabilized by intramolecular distortions (in a "large- $U$ " picture; see discussion below). The intramolecular distortion suggests a view of this system as consisting of pairs of dimers, each containing one unpaired electron. A second way of describing this material would be to view it as built from tetramers, four molecules sharing two electrons. This more complicated view allows Coulomb correlation ef-

fects to be considered. In this paper we describe the transport and optical properties of  $(\text{Me}_2\text{Fc})(\text{TCNQ})_2$ . These measurements allow us to investigate the role of electron-electron and electron-phonon interactions in this material.

### II. EXPERIMENTAL RESULTS

#### A. Transport measurements

Four-probe electrical conductivity measurements are shown in Fig. 1. The conductivity decreases smoothly from its 300-K value of  $0.03\text{-}\Omega^{-1}\text{cm}^{-1}$  when temperature is decreased. The conductivity is well fit by decomposing it into the product of mobility  $\mu$  (varying as  $T^{-\alpha}$ ) and carrier concentration (exponentially activated)

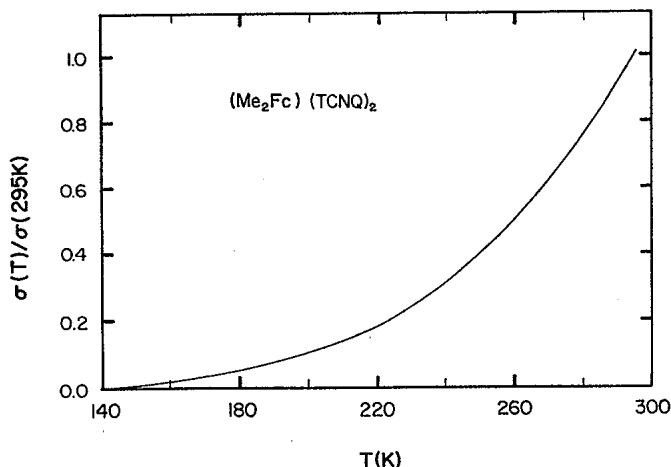


FIG. 1. dc conductivity of  $(\text{Me}_2\text{Fc})(\text{TCNQ})_2$  vs temperature.

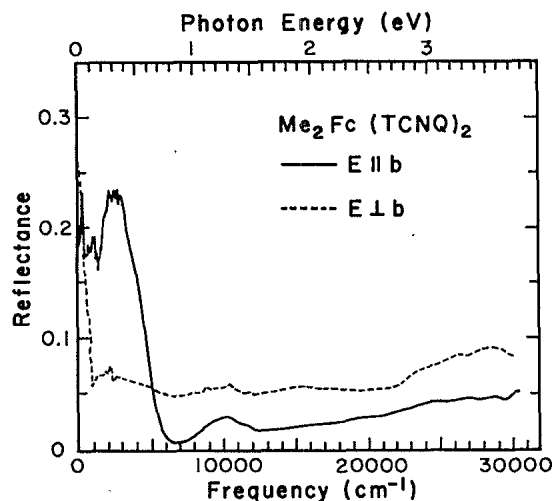


FIG. 2. Polarized reflectance of  $(\text{Me}_2\text{Fc})(\text{TCNQ})_2$  at room temperature for polarization parallel (solid line) and perpendicular (dashed line) to the stacking axis.

$$\sigma = e\mu n_0 e^{-\Delta/kT}, \quad (1)$$

where  $\Delta$  is the half gap.<sup>2,3</sup> The data of Fig. 1 yield  $2\Delta = 0.2$  eV ( $1600$   $\text{cm}^{-1}$ ) when we take<sup>2,3</sup>  $\alpha = 4$ .

### B. Optical measurements

Polarized reflectance measurements have been made on single crystals of  $(\text{Me}_2\text{Fc})(\text{TCNQ})_2$  at room temperature. The apparatus and techniques have been described previously.<sup>4</sup> Figure 2 shows the far infrared ( $20$   $\text{cm}^{-1}/2.5$

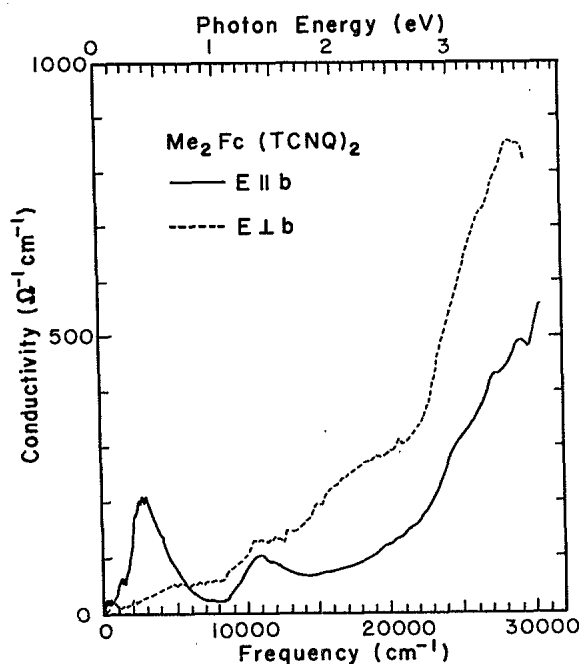


FIG. 3. Frequency-dependent conductivity obtained by Kramers-Kronig analysis of the reflectance for room temperature  $(\text{Me}_2\text{Fc})(\text{TCNQ})_2$ . The conductivity is shown parallel and perpendicular to the stacking axis.

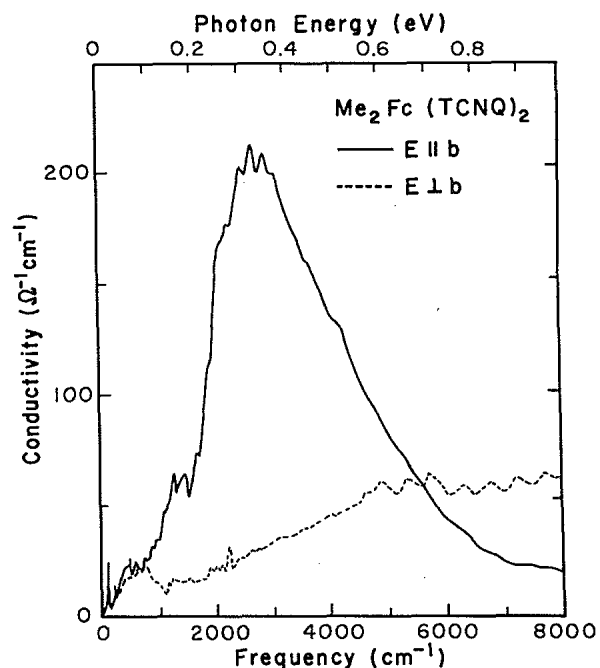


FIG. 4. Frequency-dependent conductivity at low frequencies.

meV) to ultraviolet ( $30000$   $\text{cm}^{-1}/3.7$  eV) reflectance for the electric field vector oriented parallel and perpendicular to the stacking axis. Electronic transitions in the salt cause broad maxima in the spectra while molecular vibrations lead to additional sharp features at low frequencies. With the electrical field parallel to the chain axis ( $E_{\parallel}$ ),

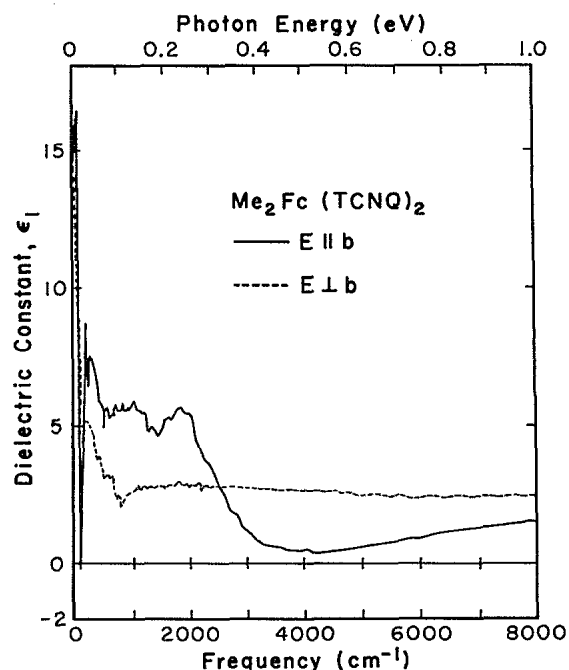


FIG. 5. Real part of the dielectric function obtained by Kramers-Kronig analysis of the reflectance for room temperature  $(\text{Me}_2\text{Fc})(\text{TCNQ})_2$ .

the reflectance extrapolates to about 30% at zero frequency. In the transverse polarization ( $E_{\perp}$ ), the reflectance is quite low throughout most of the range shown but features a sharp increase around  $1000 \text{ cm}^{-1}$  and a zero-frequency value of about 45%.

The real part of the conductivity,  $\sigma_1(\omega)$  (determined by Kramers-Kronig analysis of the reflectance), over the entire range covered is shown in Fig. 3; the low-frequency range is shown in Fig. 4. Two broad maxima in the  $E_{\parallel}$  curve are clearly present at about  $3000 \text{ cm}^{-1}$  (0.38 eV) and  $11000 \text{ cm}^{-1}$  (1.4 eV). A weak, broad maximum in the  $E_{\perp}$  reflectivity curve at  $15000 \text{ cm}^{-1}$  (2 eV) appears as a weak inflection in the conductivity curve, while the other maxima between  $23000$  and  $29000 \text{ cm}^{-1}$  (2.9–3.6 eV) are clearly seen.

The real part of the dielectric function,  $\epsilon_1(\omega)$ , is shown in Fig. 5 for the low-frequency range. For frequencies near the conductivity maxima, the dielectric function displays the usual derivativelike structure. A value of about 14 for the chain-axis dielectric constant is obtained by extrapolation to zero frequency.

### III. DISCUSSION

#### A. Electronic transitions

The electronic transitions, which we see as broad maxima in the  $\sigma_1(\omega)$  spectra, fall into two classes.<sup>5–17</sup> Those at high energies generally result from excitations of single TCNQ molecules and are called localized excitations: LE1, LE2, etc. The lower-energy bands, polarized in the stacking direction, are due to interactions among the molecules and are called charge-transfer bands: CT1, CT2, etc. The energies and oscillator strengths of these charge-transfer bands are clearly related to the electronic structure of the compound, but their interpretation may depend on whether electron-electron or electron-phonon interaction is viewed as the more important. The first view (a Hubbard picture) leads in its extreme (zero bandwidth) limit to the electrons being localized on specific sites in a Wigner lattice. The second view (a Peierls picture) leads to a distortion of the lattice and molecules with a gap opened at the Fermi surface.

#### B. Hubbard picture

For the quarter-filled-band case, such as  $(\text{Me}_2\text{Fc})\text{-}(\text{TCNQ})_2$  with electrons on average occupying every other site, it is important to consider an extended Hubbard picture,<sup>18–21</sup> which includes hopping from site to site,  $t$ , on-site Coulomb repulsion energies,  $U$ , nearest-neighbor energies,  $V_1$ , and next-nearest-neighbor energies,  $V_2$ . The Hamiltonian is

$$H = t \sum_{i,\sigma} (c_{i+1,\sigma}^{\dagger} c_{i,\sigma} + c_{i,\sigma}^{\dagger} c_{i+1,\sigma}) + U \sum_i n_{i\uparrow} n_{i\downarrow} + \frac{1}{2} V_1 \sum_i n_i (n_{i+1} + n_{i-1}) + \frac{1}{2} V_2 \sum_i n_i (n_{i+2} + n_{i-2}) \quad (2)$$

where  $i$  represents a site on the chain,  $c_{i,\sigma}^{\dagger}$  and  $c_{i,\sigma}$  are, respectively, the creation and annihilation operators for a

spin- $\sigma$  electron,  $n_{i\uparrow}$  ( $n_{i\downarrow}$ ) is the occupation-number operator for an electron of spin up (down), and  $n_i = n_{i\uparrow} + n_{i\downarrow}$  is the total number of electrons at site  $i$ .

When  $t=0$ , the problem is the distribution of  $N/2$  electrons over  $2N$  possible orbitals. This problem was solved by Hubbard<sup>18</sup> who found that the electrons arrange themselves in a generalized Wigner lattice. The electrons are highly correlated, and this correlation creates a periodic variation in charge density along the chain.

Two configurations occur for the quarter-filled-band case when  $U$  is the dominant energy (as is expected to be the case). One is a “ $4k_F$ ” structure,<sup>22</sup> which occurs when  $V_1 > 2V_2$ , whereas the other is a “ $2k_F$ ” structure,<sup>22</sup> which occurs in the opposite case. These configurations are illustrated in Fig. 6, where we have sketched the ground state and two excited states for a 12-site chain. We show a spin singlet or antiferromagnetic configuration, although Eq. (1) with  $t=0$  says nothing about the spin of singly-occupied sites. The figure gives the total energy of the eight central sites (“octet”) on the 12-site chain,  $E_{\text{oct}}$ , and the additional energy of excited-state configurations.

Optical absorption in this model occurs when an electron absorbs a photon and hops to a neighboring site. Each configuration should have two of these charge-transfer bands. The “ $4k_F$ ” configuration should have a band (CT1) at  $\hbar\omega_1 = V_1 - 2V_2$ , arising from a hop which puts an electron on a site adjacent to an occupied site, and a higher-energy band (CT2) at  $\hbar\omega_2 = U - V_2$ . As indicated in Fig. 6, this transition to a double-occupied site requires a hop to a second-nearest neighbor; thus we expect it to have substantially lower oscillator strength than CT1. The “ $2k_F$ ” configuration has a band (CT1) at  $\hbar\omega_1 = 2V_2 - V_1$  and a second (CT2) at  $\hbar\omega_2 = U - V_1$ . Because both hops are to nearest neighbors, these bands should have approximately equal oscillator strength.

The overlap or transfer integral,  $t$ , has been taken as zero in the preceding discussion, because only when  $t \ll (U, V_1, V_2)$  has the extended Hubbard model been solved analytically. As  $t$  becomes finite, it is expected

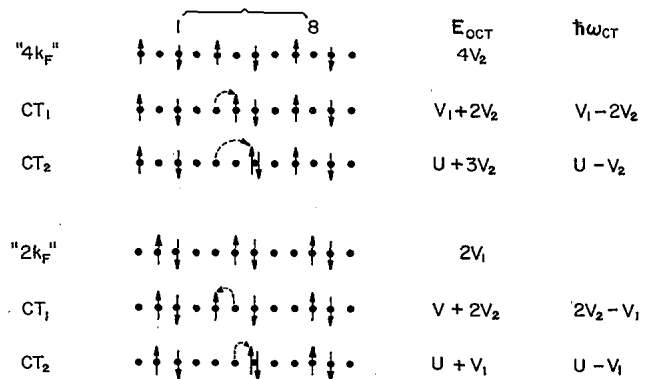


FIG. 6. Ground state and charge-transfer excitations for the quarter-filled band in “ $4k_F$ ” and “ $2k_F$ ” configurations. Occupied sites are shown as arrows, empty ones as dots. The total energy of the central 8 sites and the difference in energy between the charge transfer (CT) and ground configurations is given on the right-hand side.

that the energies of the various configurations will broaden into bands but that the picture presented above should be generally unchanged. Note that the band formed from the ground state is completely filled in the extended Hubbard model on account of the off-site Coulomb terms.

### C. Short chain models

The Hubbard model including the transfer integral can be solved for the case of chain fragments: dimers, trimers, tetramers, etc.; these solutions give indications of the properties of the infinite-length chain. The case of an isolated dimer with one electron, which has been worked out by Rice, Yartsev, and Jacobsen<sup>13</sup> and by Yartsev and Jacobsen,<sup>16</sup> could represent any two sites from the “ $4k_F$ ” structure of Fig. 6. The transfer integral term lowers the ground-state energy of the dimer by  $E_{d1} = -t$  (somewhat more if site-energy variations are included) and leads to equal probability of the electron on either site:

$$n_i \psi_i = \frac{1}{2} \psi_i. \quad (3)$$

When a chain of average occupancy  $\frac{1}{2}$  is considered, the delocalized state also has a correlation energy. Using the Hamiltonian of Eq. (2) to calculate the correlation energy for the central 8 sites of a 12-site chain in the case where  $\langle n_i \rangle = \frac{1}{2}$ , we obtain for the total energy

$$E_{\text{oct}} = -4t + 2V_1 + 2V_2, \quad (4)$$

where the factor 4 in the first term comes because the energy gain is  $-t$  per electron. We see by comparison to the  $4V_2$  energy of the “ $4k_F$ ” localized structure, the delocalized configuration would be favored if  $t > (V_1 - V_2)/2$ . Note that if the electrons are completely delocalized, there is no charge-density variation along the chain.

The dimer occupied by two electrons, which has been discussed by Rice<sup>23</sup> and by Tanner *et al.*,<sup>12</sup> should be a good model for the high-energy levels of the “ $2k_F$ ” structure of Fig. 6. This Hubbard dimer model has a ground-state energy of

$$E_{d2} = \frac{1}{2} \{ (U + V_1) - [(U - V_1)^2 + (4t)^2]^{1/2} \}. \quad (5)$$

If  $U \gg 4t$ ,  $E_{d2} = V_1 - 4t^2/(U - V_1)$ . The energy of the eight-atom segment (which contains two dimers) is

$$E_{\text{oct}} = U + V_1 - [(U - V_1)^2 + (4t)^2]^{1/2} \\ \sim 2V_1 - 8t^2/(U - V_1). \quad (6)$$

The energy gain due to the bonding interaction has the effect of reducing the nearest-neighbor repulsion energy

$$V_1 \rightarrow V_1 - 4t^2/(U - V_1). \quad (7)$$

This Hubbard dimer with two electrons has a single charge-transfer excitation polarized along the dimer axis at

$$\hbar\omega_{ct} = \frac{1}{2} \{ U - V_1 + [(U - V_1)^2 + (4t)^2]^{1/2} \} \\ \sim U - V_1 + 4t^2/(U - V_1). \quad (8)$$

This is the transition shown in the bottom row of Fig. 6.

Recently Yartsev<sup>24</sup> has worked out the charge-transfer excitations (as well as the electron-molecular vibration coupling) for the case of isolated tetramers. He includes in his Hamiltonian two transfer integrals,  $t$  and  $t'$ , on-site and nearest-neighbor Coulomb terms,  $U$  and  $V_1$ , and a site-energy difference,  $2\Delta$ , between interior and exterior members of the tetramer. Thus, his model describes highly distorted tetramers,<sup>10,13</sup> such as occur in MEM-(TCNQ)<sub>2</sub> or TEA-(TCNQ)<sub>2</sub>. He finds that there are four optically allowed transitions. When  $U/4t \gg 1$  there are two transitions at  $\hbar\omega \sim U$ , a third at  $\hbar\omega \sim V_1$ , and a fourth at lower energy which appears to be related to the site-energy difference  $\Delta$ .

### D. Peierls picture

The regular chain structure of a one-dimensional metal with finite electron-lattice coupling is unstable against a static lattice distortion. This distortion, with wave vector twice the Fermi wave vector, has the effect of opening a gap at the Fermi surface and rendering the one-dimensional chain insulating. The energy gap,  $E_g$ , is determined by the bandwidth  $4t$  and the strength of the electron-phonon coupling,  $\lambda$ ,

$$E_g = 2te^{-1/\lambda}. \quad (9)$$

This coupling is to the lattice and molecular degrees of freedom (i.e., both to acoustic phonons and intramolecular vibrations or optical phonons). The optical spectrum of the Peierls distorted metal would be that of a semiconductor, with a transition at  $\hbar\omega = E_g$ . If zone folding is important (i.e., if there is absorption involving Bragg scattering from the new, smaller Brillouin zone) there could be, for the quarter-filled case, two higher-energy transitions, with energies of order  $3t$  and  $4t$ . These should, however, be weak on account of the relatively small amplitude for scattering from the  $2k_F$  distortion.

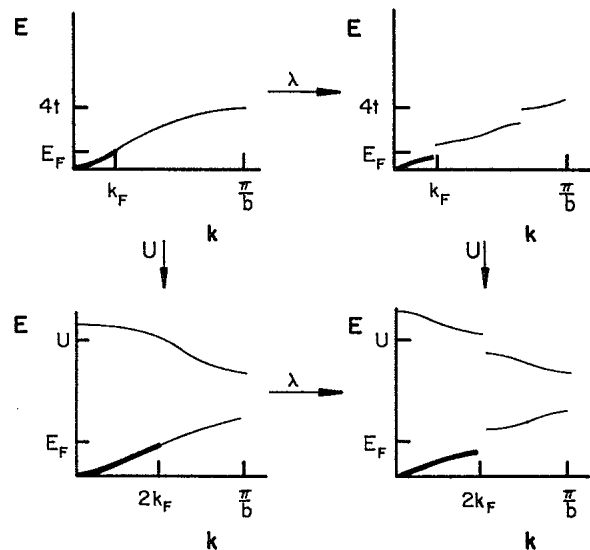


FIG. 7. Evolution of a one-dimensional metal as the electron-phonon ( $\lambda$ ) and electron-electron ( $U$ ) interactions are turned on. Wide portions of the curves show filled states.

The Peierls distortion should occur even when Coulomb interactions are important because an energy gain can still be realized by opening a Fermi-surface energy gap. If  $U$  is the dominant energy, then only single occupation of sites is allowed and the Fermi wave vector (and hence the wave vector of the lattice distortion) is twice as large as in the noninteracting case. Figure 7 shows schematically what might occur. As electron-phonon coupling ( $\lambda$ ) is turned on, a gap opens at the Fermi surface. As the on-site Coulomb interaction becomes important, half the states are raised in energy by an average amount  $U$ ; the Fermi wave vector is twice as large as before. Together the two effects produce a Peierls gap at the Fermi surface (a " $4k_F$ " distortion) and a high-lying set of states at energy  $U-4t$  above the Fermi energy.

The optical spectrum of this large- $U$  " $4k_F$ " Peierls distortion should have a transition across the Peierls gap at  $\hbar\omega = E_g$  and another transition (perhaps two) at  $\hbar\omega \sim U - 4t$ .

#### E. Localized excitons

The electronic structure of TCNQ has been studied by several investigators. Neutral TCNQ is reported<sup>7,25</sup> to have its lowest-lying electronic excitation (denoted  $LE^0$ ) at 2.8 to 3.1 eV. For  $TCNQ^-$  the extra electron occupies the lowest-lying previously empty  $\pi$  molecular orbital. Absorption spectra of solutions of TCNQ anions find<sup>5,7</sup> a low-energy excitation ( $LE1^-$ ) at 1.47 eV and a second band ( $LE2^-$ ) at 2.95 eV. Lowitz<sup>6</sup> has investigated the nature of these absorption bands through a molecular-orbital calculation of the  $\pi$ -electronic structure of  $TCNQ^0$  and  $TCNQ^-$ .

For the case of a dimer composed of two TCNQ anions, i.e., a  $(-, -)$  configuration, the interactions between the ions are observed.<sup>5,7,12</sup> The localized excitations  $LE1$  and  $LE2$  are shifted upward in energy to 1.9 and 3.3 eV, respectively, while a lower band at 1–1.4 eV is attributed to the transfer of charge between molecules (CT1). Optical studies of TCNQ salts indicate that these charge-transfer excitations are polarized along the stacking axis whereas the localized excitons are largely polarized in the transverse direction.<sup>8,11,14</sup>

#### F. Electronic transitions in $(Me_2Fc)(TCNQ)_2$

For the electric field polarized perpendicular to the stacking axis, the increasing  $\sigma_1(\omega)$  around 28 000  $cm^{-1}$  (3.5 eV) is thought to be a localized exciton  $LE2$ . A maximum is also seen at this frequency in the parallel polarization. An inflection of the  $E_{\perp}$  curve occurs at about 18 000  $cm^{-1}$  (2.2 eV) which is thought to be the localized exciton  $LE1^-$ . Note that this energy is close to the energy for  $LE1^-$  in anion dimers and much larger than the 1.5-eV energy of  $LE1^-$  in anion monomers. For the  $E_{\parallel}$  curve, two broad maxima are centered at 10 800  $cm^{-1}$  (1.3 eV) and 2700  $cm^{-1}$  (0.33 eV). The higher one is thought to be charge transfer between anions (CT2) and the lower one is charge transfer from an anion to a neutral molecule (CT1).

An estimate of the electron-energy gap is obtained from the neutral charge-transfer band centered at 2700  $cm^{-1}$ .

By extrapolating the leading edge of the band to zero conductivity, a value of 1200–1600  $cm^{-1}$  is found for the gap. This is consistent with transport measurements discussed above which give 1600  $cm^{-1}$  (0.2 eV) for the gap.

#### G. $2k_F$ or $4k_F$ ?

Two Wigner-lattice configurations occur<sup>18</sup> in the quarter-filled-band case: " $2k_F$ ", when  $V_1 < 2V_2$ , and " $4k_F$ ", when  $V_1 > 2V_2$ . The optical spectra of  $(Me_2Fc)(TCNQ)_2$  tend to support the former. The presence of a strong chain-axis band at 1.3 eV, which would be interpreted as CT2, in conjunction with a perpendicular-polarized band at 2.2 eV, which would be  $LE1$  of the  $(-, -)$  dimer, are consistent with the location of electrons on adjacent molecules. Note that the  $2k_F$  structure is a complicated one consisting of tetramers with  $(0, -, -, 0)$  charge distributions. This arrangement would have a relatively strong second harmonic  $4k_F$  component as well as the fundamental  $2k_F$  one, so it is not incompatible with an observation of a  $4k_F$  modulation of the TCNQ molecules.

It is also possible to interpret the data within a  $4k_F$  view, in which the 1.3 eV band is assigned to  $LE1^-$  of isolated ions. To explain the mostly chain-axis polarization, one must assume (1) that the tilt of the molecule relative to the chain axis enables the transition to occur and (2) that the  $E_1$  direction was nearly perpendicular to the molecule long axis. The first assumption is consistent with the observation of in-plane modes in the chain-axis vibrational spectrum (see Fig. 4 and Sec. IIIH) while the second is supported by the relatively weak vibrational features in the  $E_1$  spectrum (Fig. 4). However, it is difficult to interpret the weak band at 2.2 eV in the  $E_1$  spectrum unless it is attributed to a finite concentration of electrons on adjacent sites. (See Sec. IIIJ, below.)

A more complete measurement of the polarization dependence of the electronic bands as well as a calculation which includes not only the unpaired electrons of the ions but also the electrons which give rise to  $LE1$  is necessary before an unambiguous interpretation of the electronic spectra can be made.

#### H. Vibrational modes

The far to mid-infrared spectrum of  $(Me_2Fc)(TCNQ)_2$  shows a series of sharp absorption bands (Fig. 4). Several of these bands are attributed to the Rice effect: the totally symmetric ( $a_g$ ) vibration modes become infrared active through coupling to the conduction electrons. Note that the strength of these modes is weaker than in other quarter-filled-band TCNQ compounds, such as<sup>10</sup>  $TEA(TCNQ)_2$ . Table I lists the assignments of the observed vibrational modes. The first column gives the symmetry species, the second gives the vibrational mode, the third observed frequency, and the fourth the strength. The following column gives the frequencies as calculated or observed by Bozio *et al.*<sup>26</sup> for  $TCNQ^0$  and  $TCNQ^-$  where the notation 0 or  $(-)$  is used to label the vibrational mode. The final column lists whether the mode was observed in the parallel or perpendicular polarization of the electric field. The  $a_g$  frequencies for  $\nu_1$  and  $\nu_2$  were

TABLE I. Normal modes of  $(\text{Me}_2\text{Fc})(\text{TCNQ})_2$ .

Symmetry species	Vibrational mode	Experimental ( $\text{cm}^{-1}$ )	Strength <sup>a</sup>	Theory ( $\text{cm}^{-1}$ )	Polarization
$a_g$	$\nu_1^-$	3002	$w$	3052	parallel
	$\nu_2^-$	2287	$w$	2186	parallel
		2200			perpendicular
	$\nu_3^-$	1662	$w$	1589	parallel
	$\nu_4^-$	1435	$m$	1403	parallel
	$\nu_5^-$	1243	$m$	1206	parallel
	$\nu_6^-$	940	$w$	954	parallel
	$\nu_7^-$	670	$w$	742	parallel
$b_{1u}$	$\nu_{20}^-$	1512	$vw$	1504	perpendicular
$b_{3u}$	$\nu_{50}^0$	850	$w$	859	parallel, perpendicular
	$\nu_{50}^-$		$w$	836	
	$\nu_{51}^-$	574	$w$	585	parallel
	$\nu_{52}^-$	480	$m$	485	parallel
	$\nu_{52}^0$		$m$	475	
	$\nu_{53}^-$	222	$m$	225	parallel
	$\nu_{53}^0$		$m$	220	
		$\nu_{54}^0$	106	$s$	103

<sup>a</sup>Here  $s$  stands for strong,  $m$  for medium,  $w$  for weak, and  $vw$  for very weak.

taken as minima because the  $a_g$  modes above the gap, which is estimated to be  $1600 \text{ cm}^{-1}$ , are expected to be seen as antiresonances or dips in the spectrum.<sup>27,28</sup> Observation of mode  $\nu_6$  is doubtful; although there is a peak at the correct frequency, it may be due to noise. The modes  $\nu_8$ ,  $\nu_9$ , and  $\nu_{10}$  are not observed here.

The  $b_{3u}$  modes are out-of-plane vibrations and are expected to be observed only for the  $E_{||}$  spectrum, although some of these modes are also observed for the  $E_{\perp}$  spectrum. Similar observations are made on the  $a_g$  mode  $\nu_2^-$  which appears in both polarizations. The  $b_{1u}$  mode being an in-plane vibration is correctly observed only for the  $E_{\perp}$  spectrum. The mixing of perpendicular and parallel vibrations might be explained by the fact that the angle between the normal to the plane of the TCNQ molecule and the stacking axis<sup>1</sup> is  $14.2^\circ$  so that there are components of the electric field vector both in the molecular plane and normal to it.

Additionally, in the region  $1880\text{--}4000 \text{ cm}^{-1}$ , we find a series of peaks or weak inflections spaced approximately  $200 \text{ cm}^{-1}$  apart. This periodic structure, which is not due to interference fringes from multiple reflections between the front and back surfaces of the crystal salt (because the thickness of the sample was about  $0.01 \text{ cm}$ , whereas the absorption coefficient was about  $4 \times 10^4 \text{ cm}^{-1}$ ), may be vibronic in origin.

### I. Electron-molecular vibration coupling

The  $a_g$  modes are present in the infrared spectrum on account of the strong coupling of these vibrations to the electron density. In comparison to other quarter-filled-band TCNQ salts, for example,  $\text{TEA}(\text{TCNQ})_2$  (Refs. 10 and 29),  $(N\text{-methyl-}N\text{-ethyl)morpholinium}(\text{TCNQ})_2$  [ $\text{MEM}(\text{TCNQ})_2$ ] (Refs. 13 and 16) and  $\text{MNEB}(\text{TCNQ})_2$  (Ref. 29), these modes are much less prominent in  $\text{Me}_2\text{Fc}(\text{TCNQ})_2$ . This difference occurs even though the

electronic spectra of the four compounds are rather similar. In the remainder of this section we compare the data to models for the Rice effect which consider isolated dimers: a  $4k_F$  configuration with one electron on two sites,  $(0, -)$  or  $(-, 0)$ , and a  $2k_F$  one with two electrons on adjacent sites,  $(-, -)$ .

Rice *et al.*<sup>13</sup> have developed an expression for the frequency-dependent conductivity for noninteracting dimers with one electron per two TCNQ molecules, i.e.,  $\rho = \frac{1}{2}$ . The theory uses the overlap matrix element or transfer integral  $t$  which represents the overlap of electronic wave functions within the dimer, the charge-transfer excitation  $\omega_{\text{CT}}$  which represents the energy required to move the electron from one monomer to the other within the dimer, and a function  $D(\omega)$  which describes the effects arising from the coupling of the unpaired electron to the internal vibrations of the TCNQ molecules. The frequency-dependent conductivity is

$$\sigma(\omega) = -\frac{i\omega e^2 a^2 N}{4\Omega} \frac{\chi(\omega)}{1 - D(\omega)\chi(\omega)/\chi(0)}, \quad (10)$$

where  $\Omega$  denotes the volume of the system,

$$\chi(\omega) = \frac{8t^2/\omega_{\text{CT}}}{\omega_{\text{CT}}^2 - \omega^2 - i\omega\gamma_e} \quad (11)$$

is the reduced electronic polarizability and

$$D(\omega) = \sum_n \frac{\lambda_n \omega_n^2}{\omega_n^2 - \omega^2 - i\omega\gamma_n}, \quad (12)$$

where  $\omega_n$  is the  $n$ th phonon band ( $n = 1, 2, \dots, G$ ) for the  $G$  totally symmetric vibrational modes,  $\gamma_e$  and  $\gamma_n$  denote the natural linewidths of the originally uncoupled charge-transfer band and the phonon band  $n$ , and

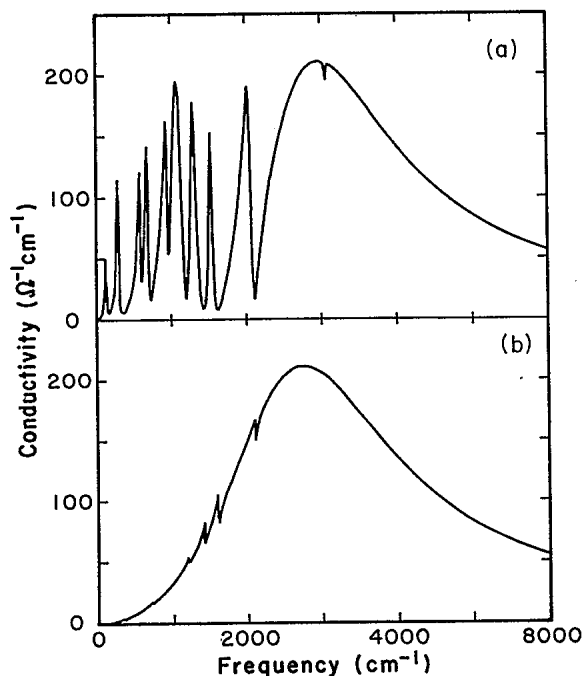


FIG. 8. Theoretical frequency-dependent conductivity for  $(\text{Me}_2\text{Fc})(\text{TCNQ})_2$  due to electron-molecular vibration coupling (a): “ $4k_F$ ” configuration; one electron on two sites. (b) “ $2k_F$ ” configuration; two electrons on two sites.

$$\lambda_n = \chi(0) \frac{g_n^2}{\omega_n} = \frac{8t^2 g_n^2}{\omega_{\text{CT}}^3 \omega_n}, \quad (13)$$

where  $g_n$  are the electron-phonon coupling constants. This model has been used to describe (*N*-methyl-*N*-ethyl)morpholinium-(TCNQ)<sub>2</sub> [MEM(TCNQ)<sub>2</sub>] in the range 20–335 K in which the TCNQ chains are strongly dimerized.<sup>13</sup>

A fit of this model to the data is shown in Fig. 8(a). The phonon frequencies and the electron phonon coupling constants used were the universal ones of Painelli *et al.*<sup>30</sup> These quantities are given in the second and third column of Table II. The values used for the other quantities are  $\gamma_n = 15 \text{ cm}^{-1}$ ,  $\omega_{\text{CT}} = 2750 \text{ cm}^{-1}$ ,  $t = 1600 \text{ cm}^{-1}$ , and

$\gamma_e = 2880 \text{ cm}^{-1}$ . The value for  $\omega_{\text{CT}}$  was chosen to be the center of the low-energy charge-transfer band;  $\gamma_e$  gave the proper width; and  $t$  was chosen to give the experimental peak height for the band. The dimensionless electron-phonon coupling constants for this  $4k_F$  situation, calculated from Eq. (13), are listed in the fourth column of Table II.

When compared to the chain-axis frequency-dependent conductivity (Fig. 4), it is clear that the theory vastly overestimates the magnitude of the effect in this material, despite the good agreement for other quarter-filled-band TCNQ salts.<sup>13,29</sup> The reason for the failure in this case is evidently that the implicit assumption of a strong  $4k_F$  charge-density wave is incorrect. If the amplitude of the charge-density wave were much smaller—so that nearly equal charge resides on every site—then the effect should in turn be reduced. This reduction occurs because the  $a_g$  modes gain their infrared intensity through modulation of the charge density on the molecules, either by shifting the charge-density-wave phase or by pumping charge back and forth between neighboring molecules. In the uniform charge-density case, neither form of modulation can occur.

To consider the  $2k_F$  case, we assume that the important sites are the two adjacent charged molecules, (–, –) and that the characteristic CT2 energy is given by Eq. (8). We further assume that the CT1 band (although present in the spectrum) does not couple to the molecular vibrations. With these assumptions, the dimensionless electron-phonon coupling constants are given by

$$\lambda_n = \frac{8t^2 g_n^2}{\omega_n [U - V_1 + 4t^2 / (U - V_1)^3]}. \quad (14)$$

The conductivity, calculated from Eqs. (10)–(12) and (14), is shown in Fig. 8(b). We used  $U - V_1 = 10500 \text{ cm}^{-1}$  (1.3 eV); the other parameters were the same as for Fig. 8(a). We now obtain a calculated conductivity reasonably resembling the experimental one, Fig. 4. The coupling constants calculated from Eq. (14) are given in the right-most column of Table II.

In this second case, we have made the assumption that the coupling constants are governed by the effective on-site Coulomb energy  $U - V_1$  and not the low-energy CT1

TABLE II.  $a_g$  mode coupling constants.

Mode	$\omega_n$ (cm <sup>-1</sup> )	$g_n$ (cm <sup>-1</sup> )	$\lambda_n$ (“ $4k_F$ ”)	$\lambda_n$ (“ $2k_F$ ”)
1	3070	40	0.0004	
2	2110	380	0.062	0.00089
3	1603	480	0.130	0.00188
4	1423	450	0.129	0.00186
5	1200	290	0.063	0.00091
6	960	125	0.015	0.00021
7	715	200	0.051	0.00073
8	602	120	0.022	0.00031
9	334	225	0.137	0.00198
10	147	110	0.074	0.00107
Total			0.683	0.00984

excitation. Recently Painelli and Girlando<sup>31</sup> have considered the situation where there are two CT excitations and have shown that the two coupling constants subtract in determining the infrared intensity of the  $a_g$  modes. Thus, the effective dimensionless electron-phonon coupling constant should be the difference between the " $4k_F$ " and the " $2k_F$ " terms in Table II. However, as the former are so much larger than the latter the result for the conductivity would be indistinguishable from Fig. 8(a), and not in agreement with experiment. Thus there must be an actual cancellation (probably on account of the uniform molecular spacing, as recently discussed by Painelli and Girlando<sup>31</sup>) of the contribution of the low-energy CT1 transition.

### J. Solitons

Rice and Mele<sup>32</sup> have predicted that large  $U$ , quarter-filled-band systems (with a " $4k_F$ " configuration) can support the formation of solitons by thermal processes or by chemical doping. The presence of such states would lead to intragap absorption processes. As shown in Fig. 4, we do observe an absorption at frequencies below the gap ( $E_g \sim 1600 \text{ cm}^{-1}$ ). The onset of absorption well below the gap and the continued increase with frequency to well past the band edge are also seen in TTF-TCNQ and other

TCNQ compounds.<sup>33</sup> The origin of the absorption below the gap may be partly due to solitons.<sup>3</sup> The band at 2.2 eV in the  $E_1$  spectrum is also consistent with the presence of solitons.

### IV. CONCLUSION

In conclusion, by measuring the optical properties of  $(\text{Me}_2\text{Fc})(\text{TCNQ})_2$ , we have examined several important interactions involving the unpaired electrons on the TCNQ chains. The excitation energies have been estimated and the electron-molecular-vibrational coupling has been studied. The existence of a Peierls gap has been established from the infrared data. From analysis of the charge-transfer excitations we have estimated the on-site Coulomb interaction ( $U$ ) and the transfer matrix element ( $t$ ). Since  $U > 4t$  the Coulomb interactions are strong and the electrons are "localized" on the TCNQ molecules.

### ACKNOWLEDGMENTS

This research was supported by the National Science Foundation Grants No. DMR-8218021 and DMR-8416511. D.B.T. would like to thank C. S. Jacobsen for discussions about  $2k_F$  and  $4k_F$  distortions in large  $U$  systems.

- <sup>1</sup>S. R. Wilson, P. J. Corvan, R. P. Seiders, D. J. Hodgson, M. Brookhart, W. E. Hatfield, J. S. Miller, A. H. Reis, P. K. Rogan, E. Gebert, and A. J. Epstein, in *Molecular Metals*, edited by W. E. Hatfield (Plenum, New York, 1979), p. 407. TCNQ is  $\text{C}_{12}\text{H}_4\text{N}_4$  or 2,2'-(2,5-cyclohexadiene)bis(propanedinitrile-2-ylidene).
- <sup>2</sup>A. J. Epstein and E. M. Conwell, *Solid State Commun.* **24**, 627 (1977).
- <sup>3</sup>A. J. Epstein, E. M. Conwell, D. J. Sandman, and J. S. Miller, *Solid State Commun.* **23**, 355 (1977).
- <sup>4</sup>K. D. Cummings, D. B. Tanner, and J. S. Miller, *Phys. Rev. B* **24**, 4142 (1981).
- <sup>5</sup>R. H. Boyd and W. D. Phillips, *J. Chem. Phys.* **43**, 2927 (1965).
- <sup>6</sup>D. A. Lowitz, *J. Chem. Phys.* **46**, 4698 (1967).
- <sup>7</sup>Y. Iida, *Bull. Chem. Soc. Jpn.* **42**, 71 (1969).
- <sup>8</sup>J. Tanaka, M. Tanaka, C. Tanaka, T. Ohno, T. Takabe, and H. Anzai, *Ann. Sci.* **313**, 256 (1978).
- <sup>9</sup>J. B. Torrence, B. A. Scott, and F. B. Kaufman, *Solid State Commun.* **17**, 1369 (1975).
- <sup>10</sup>A. Brau, P. Breusch, J. P. Farges, W. Hina, and D. Kuse, *Phys. Status Solidi B* **62**, 615 (1974). TEA is an abbreviation for triethylammonium.
- <sup>11</sup>D. B. Tanner, C. S. Jacobsen, A. A. Bright, and A. J. Heeger, *Phys. Rev. B* **16**, 3238 (1977).
- <sup>12</sup>D. B. Tanner, J. S. Miller, M. J. Rice, and J. J. Ritsko, *Phys. Rev. B* **21**, 5835 (1980).
- <sup>13</sup>M. J. Rice, V. M. Yartsev, and C. S. Jacobsen, *Phys. Rev. B* **21**, 3437 (1980). MEM is an abbreviation for (*N*-methyl-*N*-ethyl)morpholinium.
- <sup>14</sup>K. Yakushi, M. Iguchi, G. Katagiri, T. Kusaka, T. Ohta, and H. Kuroda, *Bull. Chem. Soc. Jpn.* **54**, 348 (1981).
- <sup>15</sup>J. Tanaka, M. Tanaka, T. Kawai, T. Takaba, and O. Maki, *Bull. Chem. Soc. Jpn.* **49**, 2358 (1976).
- <sup>16</sup>V. M. Yartsev and C. S. Jacobsen, *Phys. Rev. B* **24**, 6167 (1981).
- <sup>17</sup>D. B. Tanner, in *Extended Linear Chain Compounds*, edited by Joel S. Miller (Plenum, New York, 1982), Vol. 2.
- <sup>18</sup>J. Hubbard, *Phys. Rev. B* **17**, 494 (1978).
- <sup>19</sup>S. Mazumdar and Z. G. Soos, *Phys. Rev. B* **23**, 2810 (1981).
- <sup>20</sup>S. Mazumdar and A. N. Bloch, *Phys. Rev. Lett.* **50**, 207 (1983).
- <sup>21</sup>J. E. Hirsch and D. J. Scalapino, *Phys. Rev. Lett.* **50**, 1168 (1983).
- <sup>22</sup>If there are on average  $\rho < 2$  electrons per TCNQ molecule ( $\rho = \frac{1}{2}$  in the quarter-filled-band case), then, because each orbital can hold two electrons, a tight-binding, noncorrelated model would give a metallic ground state, with a Fermi wave vector of  $k_F = \rho\pi/2b$ , where  $b$  is the spacing along the chain and the Brillouin-zone boundaries are at  $\pm\pi/b$ . The ordinary Peierls distortion occurs at  $q_p = 2k_F$ , so that  $q_p = \rho\pi/b$ . The wavelength of the distortion is  $\lambda_p = 2\pi/q_p = 2b/\rho$ . Thus a distortion with this fundamental period is called a " $2k_F$ " distortion. However, if the on-site Coulomb interaction is the dominant energy (i.e., if  $U > 4t$ ), there is then only single occupancy of the orbitals; the Fermi wave vector is  $\rho\pi/b$ . A Peierls distortion would still occur at twice this Fermi wave vector, i.e., at  $q_{ph} = 2\rho\pi/b$ . This distortion is, thus, at  $q_{ph} = 4k_F$  ( $k_F$  is defined to equal its value in the noninteracting case) and has a period  $\lambda_{ph} = b/\rho$ . The presence of such a " $4k_F$ " distortion is usually taken as evidence for strong Coulomb interactions. For the case considered here,  $\rho = \frac{1}{2}$ , we have  $k_F = \pi/4b$ ,  $2k_F = \pi/2b$ ,  $\lambda_p = 4b$ ,  $4k_F = \pi/b$ ,  $\lambda_{ph} = 2b$ .
- <sup>23</sup>M. J. Rice, *Solid State Commun.* **31**, 93 (1979).
- <sup>24</sup>V. M. Yartsev, *Phys. Status Solidi B* **126**, 501 (1984).
- <sup>25</sup>R. R. Pennelly and C. J. Eckhardt, *Chem. Phys.* **12**, 89 (1976).



- <sup>26</sup>R. Bozio, I. Zanon, A. Girlando, and C. Pecile, *J. Chem. Soc. Faraday Trans.* **174**, 235 (1978).
- <sup>27</sup>U. Fano, *Phys. Rev.* **124**, 1866 (1961).
- <sup>28</sup>M. J. Rice, L. Pietronero, and P. Brüesch, *Solid State Commun.* **21**, 575 (1977).
- <sup>29</sup>E. F. Steigmeier, H. Auderset, D. Baeriswyl, and M. Almeida, *Mol. Cryst. Liq. Cryst.* **120**, 163 (1985). MNEB is an abbreviation for methyl-*N*-ethylbenzimidazolium.
- <sup>30</sup>A. Painelli, A. Girlando, and C. Pecile, *Solid State Commun.* **52**, 801 (1984).
- <sup>31</sup>A. Painelli and A. Girlando, *J. Chem. Phys.* (to be published); A. Painelli, C. Pecile, and A. Girlando, *Mol. Cryst. Liq. Cryst.* **134**, 1 (1986).
- <sup>32</sup>M. J. Rice and E. J. Mele, *Phys. Rev. B* **25**, 1339 (1982).
- <sup>33</sup>J. E. Eldridge and F. E. Bates, *Phys. Rev. B* **28**, 6972 (1983). TTF is an abbreviation for tetrathiafulvalene, or C<sub>6</sub>H<sub>4</sub>S<sub>4</sub> with the structural formula 2,2'-*bi*(1,3-dithiole-2-ylidene).